

**\*Manuscript**[Click here to view linked References](#)**Surface energy analysis (SEA) and rheology of powdered milk dairy products**

Tubomir Lapčík<sup>1,2\*</sup>, Barbora Lapčíková<sup>1,2</sup>, Eva Otyepková<sup>1</sup>, Michal Otyepka<sup>1</sup>, Jakub Vlček<sup>1</sup>,  
František Buňka<sup>2</sup>, Richardos Nikolaos Salek<sup>2</sup>

<sup>1</sup> Department of Physical Chemistry, Regional Centre of Advanced Technologies and Materials, Faculty of Science, Palacky University, 17. listopadu 12, 77146 Olomouc, Czech Republic

<sup>2</sup> Tomas Bata University in Zlin, Faculty of Technology, Institute of Foodstuff Technology, nám. T.G. Masaryka 5555, 760 05 Zlín, Czech Republic

\*Corresponding author.

E-mail address: [lapcikli@seznam.cz](mailto:lapcikli@seznam.cz), phone: +420732506770

**Key words:** skimmed milk powder, whey powder, demineralised whey powder, wetting, surface energy distribution, surface energy analysis, inverse gas chromatography, thermal analysis, scanning electron microscopy, powder rheology, flow index

**Abstract**

Results of inverse gas chromatography adsorption/desorption experiments **using** selected probes on skimmed milk, whey and demineralised whey powder materials are presented. **The** dispersive component of surface energy **was found to be dominant, indicating** low polarity character. Surface energy profiles **of demineralised whey and skimmed milk showed a characteristic** steep exponential decrease **from** approximately 170 mJ/m<sup>2</sup> to 60 mJ/m<sup>2</sup> **and 140 mJ/m<sup>2</sup> to 45 mJ/m<sup>2</sup>, respectively, whereas whey powder exhibited a constant (non-**

26 **exponential) surface energy at** approximately 45 mJ/m<sup>2</sup>\*\*. **The** dispersive surface energy of  
27 **demineralised whey and skimmed milk powder showed a broad distribution** ranging  
28 **from 40 mJ/m<sup>2</sup> to 120 mJ/m<sup>2</sup> and 175 mJ/m<sup>2</sup>, respectively. In contrast, the dispersive**  
29 surface energy distribution for whey **was very narrow, ranging from only** 42.8 mJ/m<sup>2</sup> to 45  
30 mJ/m<sup>2</sup>. **The determined** yield locus and Mohr's circles **indicated** that demineralised whey  
31 **exhibited** free flowing powder characteristics, **whereas skimmed** milk and whey **exhibited**  
32 **cohesive powder** flow behaviour.

33

## 34 **1. Introduction**

35

36 **Powdered** milk is a major precursor for many food products. Its value has been enhanced  
37 **in recent years** by **the** relatively large amount of research **conducted to** support the  
38 development and commercialisation of dairy-based products with an increasing variety of  
39 **flavours, textures and shelf-lives** (Osorio, Monjes, Pinto, Ramirez, Simpson & Vega, 2014,  
40 Saffari & Langrish, 2014, Crowley, Gazi, Kelly, Huppertz & O'Mahony, 2014, Bolenz,  
41 Romisch & Wenker, 2014, Romeih, Abdel-Hamid & Awad, 2014, Martinez-Padilla, Garcia-  
42 Mena, Casas-Alencaster & Sosa-Herrera, 2014, Zhou, Liu, Chen, Chen & Labuza, 2014,  
43 Nilufer-Erdil, Serventi, Boyacioglu & Vodovotz, 2014). The colloidal nature of cow's milk is  
44 a crucial structural feature that affects **its** final product quality as well **as processing**  
45 behaviour (Fox & McSweeney, 1998, Gaucheron, Famelart, Mariette, Raulot, Michel &  
46 Legraet, 1997). It can be divided into two compositional **domains: the** casein micelle and the  
47 milk fat globule. These colloidal domains comprise nearly 80% of the approximate 12.7 g  
48 total solids per 100 g<sup>-1</sup> in milk. **Therefore, investigation of** the structure and interactions of  
49 these colloidal particles **continues** to be **an important area of** milk research. Dried milk  
50 powders (e.g. whole, skimmed or retentate), dried buttermilk, and other dairy **powders (e.g.**

51 cheese whey powder (WP), whey protein concentrates (WPC), whey protein isolates (WPI),  
52 caseinates and **lactose**) are products made from milk **or** whey where practically all the water  
53 is removed, i.e. to  $< 4 \text{ g per } 100 \text{ g}^{-1}$  of water (Tamime, Robinson & Michel, 2007). These  
54 dried products have a very long shelf-life, they can be stored at ambient **temperature and** can  
55 be **readily** exported to countries that have a shortfall in milk production. After rehydrating  
56 milk powders, the reconstituted products may be similar to fresh milk (whole or **skimmed**),  
57 **whereas the remaining** dairy powders have different applications in the dairy, food and  
58 pharmaceutical industries.

59 In this **study, the** term skimmed milk powder defines a dairy product obtained by  
60 removing the water from skimmed milk, with a maximum fat content of 11%, a maximum  
61 moisture content of 5% and protein content not less than 31.4% of non-fatty dry extract.  
62 Skimmed milk powder is by far the most important of **all milk powders** and the most widely  
63 used form of milk protein in the food industry. Skimmed milk production firstly involves its  
64 evaporation to a concentration of about 50% of total solids. Thereafter, the evaporated  
65 skimmed milk can be dried in any of the various types of spray drier available. Two types of  
66 powder **can** therefore **be distinguished: roller-dried powder** and spray-dried powder.  
67 **Moreover, skimmed** milk powder **represents a** significant source of protein (35%) and  
68 carbohydrate (lactose, 50%) and can be used as a food ingredient, for reconstitution and as an  
69 animal feed. **As a food ingredient, it performs** three **main** functions: (i) contributes to a  
70 desirable dairy flavour, (ii) affects food **texture, and** (iii) enhances the development of  
71 desirable colour and flavour compounds (Tamime, Robinson & Michel, 2007, **Ranken, Kill**  
72 **& Baker**, 1997).

73 Whey is a general term describing the translucent liquid part of milk that remains  
74 following the process (isoelectric or rennet coagulation) of cheese manufacturing (Hoffman  
75 & Falvo, 2004, Manso & Lopez-Fandino, 2004). Whey prepared by isoelectric precipitation

76 or rennet coagulation is called acid whey (dry whey with **0.35%** or higher titratable acidity on  
77 a reconstituted basis) **or** sweet (rennet) whey (dry whey not over **0.16%** titratable acidity on a  
78 reconstituted basis), respectively. Whey contains nearly 50% of the total solids found in  
79 whole milk, including essentially **all the** lactose and whey proteins (Fundamentals of cheese,  
80 15). The content of total essential amino acids and branched-chain amino acids is **high** in  
81 whey protein than in most **other** dietary proteins (Helaine, Valdemiro, Dias, Borges, &  
82 Tanikawa, 2001). Whey and whey products are commonly used in animal feed, dietetic foods  
83 (infant food), bread, confectionery, candies and beverages. The composition of whey products  
84 varies depending on several factors, including the source of the milk, production method, type  
85 of cheese and manufacturer's specifications. Whey and whey components contain a number  
86 of valuable minerals **such as calcium, magnesium, manganese, phosphorus, copper, iron,**  
87 **zinc, sodium and potassium.**

88         The main component of whey is lactose (**70-75%**), **while** the major component of  
89 whey solids **are** whey proteins (**10-13%**), **mainly** lactalbumin and globulins. Practically all  
90 the mineral elements found in whey are essential for nutrition. Condensed whey, dried whey,  
91 dried modified whey, whey protein concentrate and isolates, as well as lactose (**crystallised**  
92 and dried) are the **most** often **reported** whey products. Whey can also be processed into a  
93 number of valuable **products**, as well as some that are considered waste products. **Examples**  
94 **of** whey types include reduced lactose whey, demineralised whey, acid **whey**, **sweet** whey and  
95 whey protein concentrate. Whey protein is a complete, high quality protein with a rich amino  
96 acid profile. Whey proteins refer to a group of individual proteins or fractions that separate  
97 out **from casein** during cheese-making. These fractions are **usually** purified to different  
98 **concentrations depending** on the end composition desired **and vary** in their content of  
99 protein, lactose, carbohydrates, **immunoglobulins**, minerals and fat (Tamime et al., 2007).

100 Demineralised whey powder is produced from whey by selective removal of most of the  
101 minerals.

102 The properties of surfaces and interfaces **characterised** by surface or interfacial  
103 tension and surface energy **have attracted increasing attention** in recent years. **Such**  
104 properties **affect** many phenomena **associated with** adhesion, wetting, spreading and  
105 **wicking, which play an important role in everyday** life, natural processes **and numerous**  
106 industrial applications. These processes **are important in** various **materials, for** instance  
107 biopolymers (Lapčik, Lapčik, De Smedt, Demeester & Chabreček, 1998, Collins, 2014),  
108 synthetic polymers, wood (Lapčik, Lapčik, Kubiček, Lapčíková, Zbotil & Nevečná, 2014),  
109 paper, stone, soils (Lapčik, Lapčíková, Krásný, Kupská, Greenwood & Waters, 2012),  
110 cereals and **textiles, encompassing** all possible types of surface **from polar to non-polar**  
111 **(Gamble et al., 2012). However, the surfaces of such materials are usually rough rather**  
112 **than smooth and may even be porous, making their surface characterisation challenging.**  
113 Despite the **difficulties, several methods are applicable for characterising** powder and  
114 fibrous materials (Gajdošíková, Lapčíková & Lapčik, 2011), such as **the** capillary rise  
115 method, thin-layer wicking **and Wilhelmy** plate method. **In particular, a surface energy**  
116 analysis technique based on inverse gas chromatography has been found to be very effective  
117 **for characterising** wetting phenomena on powders and fibres (Mohammadi-Jam & Waters,  
118 2014, Lapčik, Otyepková, Lapčíková & Otyepka, 2013, Lazar, P. et al., 2014)

119

120

## 121 **2. Methods**

### 122 ***2.1.Theoretical background***

123 **The surface** free energy of a solid can be described **by** the sum **of dispersive** and  
124 specific contributions. Dispersive (apolar) interactions, also known as Lifshitz-van der Waals

125 interactions, consist of London **interactions originating** from electron density changes but  
 126 may **also** include both Keesom and Debye interactions (Gajdošíková et al, 2011). Other forces  
 127 influencing the magnitude of surface energy are Lewis acid-base **interactions, which** are  
 128 generated between **an** electron acceptor (acid) and electron donor (base). They **occur in**  
 129 **compounds** containing hydrogen bonds - strong secondary bonds between atoms of hydrogen  
 130 and a highly electronegative element such as F, O, N and Cl or other compounds **that can**  
 131 **interact with** Lewis acids and bases. Details of the **most** widely accepted theoretical  
 132 treatment **for estimation** of solid surface free **energies from** selective wetting measurements  
 133 are **given** in our **recent** review article (Gajdošíková et al., 2011).

134 The dispersive component of the surface energy  $\gamma_S^D$  can be calculated from the  
 135 retention **times** obtained from inverse gas chromatography measurements of a series of n-  
 136 alkane probes injected at infinite dilution (concentration within the **Henry region** of the  
 137 adsorption **isotherm**) (Belgacem, Gandini & Pefferkorn, 1999). For evaluation of these  
 138 **dependencies, two approaches have been used, as described by Equations (1)** (Schultz,  
 139 Lavielle & Martin, 1987) **and (2) (Dorris & Gray, 1980):**

140

$$141 \quad RT \ln V_N = a (\gamma_L^D)^{1/2} 2N_A (\gamma_S^D)^{1/2} + C \quad (1)$$

142

143 where  $R$  is the universal gas constant,  $N_A$  is Avogadro's number,  $\gamma_L^D$  is the dispersive  
 144 component of surface free energy of the liquid probe,  $\gamma_S^D$  is the dispersive component of the  
 145 surface free energy of the solid,  $V_N$  is the retention volume and  $C$  is a constant, and

146

$$147 \quad \gamma_S^D = \frac{RT \ln \left( \frac{V_{N(C_nH_{2n+4})}}{V_{N(C_nH_{2n+2})}} \right)}{4 N_A^2 a_{CH_2}^2 \gamma_{CH_2}} \quad (2)$$

148

149 where  $a_{\text{CH}_2}$  is the surface area of a  $\text{CH}_2$  unit ( $\sim 0.6 \text{ nm}^2$ ) and  $\gamma'_{\text{CH}_2}$  is its free energy  
150 (approximately **35.6 mJ/m<sup>2</sup>**).

151

## 152 ***2.2.Experimental***

153

154 Inverse gas chromatography was conducted using a **surface energy analyser** (SEA) (Surface  
155 Measurement Systems, UK). Samples were placed in 4 mm (internal diameter) **columns to**  
156 give a total surface area of approximately  $0.5 \text{ m}^2$ . The following eluent vapours were passed  
157 through the column: **nonane, octane, hexane and heptane**. All reagents were obtained from  
158 Sigma Aldrich (**USA**) and were of analytical grade. The injection of vapours was controlled  
159 **in order** to pass a set volume of eluent through the column to give pre-determined fractional  
160 coverage of the sample in the column. **Using this method, the** retention time of the vapours  
161 **through** the particles gives an indication of the surface properties of the material, including  
162 the surface energy. By gradually increasing the amount of vapour injected, it is possible to  
163 build up a surface heterogeneity plot.

164 Specific surface area measurements were made using a Micromeritics TriStar 3000  
165 surface area and porosity analyser (USA) **combined with** the nitrogen BET technique.

166 Thermogravimetry (TG) and differential thermal analysis (DTA) experiments were  
167 performed on a Netzsch STA 449 C Jupiter **simultaneous thermal analyser** (Netzsch,  
168 Germany). **Samples were weighted to aluminium pans and measured. Each measurement**  
169 **was repeated 3 ×. Conditions of measurement: Heat flow 10 °C/min and dynamic**  
170 **atmosphere of nitrogen (N<sub>2</sub> 50 ml/min), range of temperature measurement was from**  
171 **35 °C to 300 °C**. Throughout the experiment, the sample temperature and weight-heat flow  
172 changes were continuously monitored.

173 Scanning electron microscopy (SEM) images were captured on a Hitachi 6600 FEG  
174 microscope (Japan) operating in the secondary electron mode and using an accelerating  
175 voltage of 1 kV.

176 Powder rheology measurements were **acquired** on a FT4 Powder rheometer (Freeman  
177 Technology, UK). All experiments were performed **under the** laboratory ambient  
178 temperature of **23 °C** and air relative humidity of **43%**.

179 **The moisture content of the powdered samples was as follows:** skimmed **milk 3.7**  
180 **wt.%, whey 2.0 wt.% and demineralised whey 2.4 wt.%** (Moravia Lacto, Czech  
181 Republic). **The powdered** milk samples were **stored under** dry conditions in desiccators (at  
182 **an ambient temperature of 23 °C**) for 2 weeks prior to **the** experiments.

183

### 184 **3. Results and discussion**

185

186 A typical SEM **image for the powdered** milk materials under study **is presented** in  
187 Figure 1, **showing that the particles had a spherical shape. The** individual **particle**  
188 diameter of **the powdered** skimmed milk **sample** was found to be 15.1  $\mu\text{m}$ , **compared to**  
189 80.0  $\mu\text{m}$  and **88.0  $\mu\text{m}$**  for **the powdered whey and** demineralised whey **samples,**  
190 **respectively.** All samples were characterised by thermogravimetric and DSC measurements  
191 **over a** temperature range of +35 to +300 °C to evaluate moisture content and thermal  
192 stability. **The observed** TG and DSC temperature dependencies are shown in Figures 2 and 3.  
193 **It can be seen from these scans (Figure 2) that the powdered** skimmed milk **and whey**  
194 samples **exhibited** three step weight loss patterns. **The first** TG weight loss step **occurred**  
195 **from 35 to 150 °C and corresponded to a** weight loss of 4.6 **wt.%** for **the** skimmed milk  
196 **and 3.1 wt.%** for **the whey sample, representing** moisture release of physically retained  
197 water molecules by casein or whey proteins. **As** all samples were conditioned **at the same**



198 **humidity** prior to the experiments, **the** linear zero moisture behaviour in the case of  
199 demineralised whey **is likely due** to its low **mineral** content in comparison to the other two  
200 materials (**skimmed** milk and whey). **The second** TG degradation step **occurring over the**  
201 **temperature range 150 to 248 °C** was **attributed** to the thermo-destruction of casein and  
202 whey **proteins** (Mocanu, Moldoveanu, Odochian, Paius, Apostolescu & Neculau, 2012). The  
203 thermal stability of **the** studied milk dairy products **can be described** by the initial  
204 temperature of thermal degradation (**2. region**), **which was** 150 °C. **At this temperature, the**  
205 weight loss for all samples was approximately 25 to 32 **wt.%**. The third degradation step was  
206 initiated at 248 °C for **skimmed** milk and whey and at 236 °C for demineralised whey. **The**  
207 residual masses were 62.9 **wt.%** for **powdered** skimmed milk, 56.9 **wt.%** for **powdered**  
208 whey and 60.9 **wt.%** for demineralised **powdered** whey. As evident from Figure 2, the  
209 weight lost **pattern** of skimmed milk **during the third degradation step** was inverted  
210 (**became** the lowest) in comparison to the first and second degradation regions. We ascribed  
211 this behaviour to the higher residual mass of lactose in comparison to the milk fats. **The**  
212 **thermal** characteristics of milk powder are significantly affected by fat and lactose content  
213 (**Rahman, Al-Hakmani, Al-Alawi & Al-Marhubi**, 2012). However, the tangent of the  
214 sample weight at 200 °C **was** higher for the whey products in comparison to the skimmed  
215 milk, **indicating that milk fats have a** lower degradation **resistivity in** comparison **to lactose**  
216 **in** skimmed milk. **As milk** is a multi-component **mixture, it** would be difficult to **attribute**  
217 its thermal **behaviour to particular** components **as** complex individual as well as synergistic  
218 effects **need to be taken into account**.

219 Based on **the** DSC data (Figure **3**), **the** first exothermic peak at approximately 170 °C can  
220 be **assigned to lactose crystallisation** and **the** second **huge peak** to the non-enzymatic  
221 browning advanced Maillard reaction between proteins and **lactose, which is** initiated at a  
222 temperature of 220 °C (Vuataz, Meunier & Andrieux, 2010, **Rahman et al.**, 2012)). The last

223 third degradation region **is likely to correspond to oxidation** of milk fats **and lactose**  
224 degradation (Raemy, Hurrell & Löliger, 1983).

225 **The specific** surface areas of the studied samples were identical for all materials under  
226 **study. Although the** obtained value of  $0.6 \text{ m}^2/\text{g}$  was relatively low, **it was** in excellent  
227 agreement **with data** available in **previous** literature (Berlin, Howard & Pallansch, 1964).

228 Surface energy profiles and their components of **the** studied milk products powders based  
229 on **the** inverse gas chromatography **measurements are** shown in Figure 4. **The** surface  
230 energy profiles of **skimmed** milk and demineralised whey **clearly differed from that of**  
231 **whey. The** first two materials (**skimmed** milk and demineralised whey) **showed a**  
232 **characteristic steep** exponential decrease in surface energy **from approximately  $170 \text{ mJ/m}^2$**   
233 **to  $60 \text{ mJ/m}^2$  and  $140 \text{ mJ/m}^2$  to  $45 \text{ mJ/m}^2$ , respectively, between a coverage of 0% to**  
234 **approximately 2% (skimmed milk) and 5% (demineralised whey), reflecting the**  
235 relatively **low** number of high energy sites **on** the surface of **these** materials. **In contrast, for**  
236 **a surface coverage of 5% up to 20%, the** surface energy **profiles plateaued** at  $45 \text{ mJ/m}^2$   
237 (**skimmed milk**) and  $60 \text{ mJ/m}^2$  (**demineralised whey**). As clearly visible from Figure 4, **the**  
238 dispersive component **dominated the** surface **energy, thus** reflecting **the** non-polar nature of  
239 the surface active sites in **both skimmed** milk and demineralised **whey powders**. The same  
240 hydrophobic character was **also found for** the third material under **study, i.e.** whey. However,  
241 in contrary to the above mentioned skim milk and demineralised whey materials, a surface  
242 energy coverage dependence exhibited stable non-exponential (linear) pattern with the  
243 magnitude of the observed surface energy approximately  $45 \text{ mJ/m}^2$ , thus reflecting high  
244 homogeneity of acting energetic surface sites\*\*. For all three tested materials, **the** polar  
245 component of the surface energy was negligible in comparison to the dispersive component.  
246 **For both the whey and demineralised whey powders, its value** was **independent of**  
247 **coverage at approximately  $5 \text{ mJ/m}^2$ , thus suggesting a** high uniformity of surface structural

248 components responsible for this kind of behaviour. **However, the polar component of**  
249 **skimmed milk showed an exponential decay, ranging from 30 mJ/m<sup>2</sup> for a coverage of**  
250 **0% coverage up to 5 mJ/m<sup>2</sup> for coverages of 3% up to 20%, which indicates a** broader  
251 distribution **of energetic** sites responsible for such behaviour due to the **increased** complexity  
252 of the main **milk constituents. It was also evident that** the polar surface active sites **were** of  
253 relatively low energy in all **the** studied powders, **providing further evidence of** their low  
254 polarity character. Such behaviour can be attributed to the presence **of milk** fat components at  
255 the surface interface (Jensen, Ferris & Lammi-Keefe, 1991).

256 **The measured** dispersive surface energy (Figure 5), **showed a characteristically** broad  
257 **distribution for both skimmed milk (40 mJ/m<sup>2</sup> to 175 mJ/m<sup>2</sup>) and demineralised whey (40**  
258 **mJ/m<sup>2</sup> to 120 mJ/m<sup>2</sup>), thus reflecting the large** number of structural elements responsible for  
259 this behaviour. **However,** the dispersive surface energy distribution **of** whey **was** very  
260 **narrow (see Figure 5 - inset), ranging from only 42.8 mJ/m<sup>2</sup> to 45 mJ/m<sup>2</sup>, with** relatively  
261 the same area increment occupancy of 2% as for demineralised whey. **In contrast, the area**  
262 increment occupancy for **skimmed** milk was 3 times **higher, reaching 6%. This SEA pattern**  
263 behaviour **may be due to** the **greater concentration** of inorganic salts in whey in comparison  
264 **to milk** and demineralised whey, which might successfully screen the most energetic **surface**  
265 **sites** (at the lowest surface coverage) by binding surrounding water molecules remaining as  
266 residual moisture content.

267 **The** macroscopic powder flow behaviour **was also investigated by determining the**  
268 yield locus and flow function dependencies at different stress levels for **the** studied **samples.**  
269 Results of the powder rheological measurements are shown in Figure 6, **which presents the**  
270 yield locus and Mohr's circles of **the** tested powder milk dairy products. **The results show**  
271 that demineralised whey exhibited free flowing powder **characteristics, as indicated by the**  
272 observed friction coefficient **of 11.7. In contrast, the friction** coefficients of **the skimmed**

273 milk and whey powders **ranged from 3.3** to 4.5, **which are** values characteristic for cohesive  
274 powders behaviour. **The** unconfined yield strengths **ranged** from 1.37 kPa (demineralised  
275 whey) to 4.48 kPa (**skimmed** milk) and 4.69 kPa (whey). The unconfined yield **strength**,  $\sigma_c$ ,  
276 **can be obtained** from the stress circle tangential to the yield locus **and passing** through the  
277 origin (minor principal stress  $\sigma_2 = 0$ ). Because the largest Mohr stress circle **indicated** a state  
278 of steady-state flow, the internal friction angle can be regarded as a measure of the internal  
279 friction at steady-state flow (**Lapčik et al.**, 2012). For **the** studied **samples**, **the** angle of  
280 internal friction **ranged** from **26.5°** for whey up to 36.4 and **40.4°** for demineralised whey and  
281 **skimmed milk, respectively**. **The** **relatively** low value of the angle of internal friction  
282 observed for whey **is consistent with** the observed friction factor of 3.3 characteristic for  
283 cohesive powders. The relevant consolidation **stress**,  $\sigma_1$ , **can be obtained from** the major  
284 principal stress of the Mohr stress **circle tangential** to the yield locus and **intersecting** the  
285 point of steady flow. **The major principle** stress for all **the** tested powders was about 16 to  
286 18 kPa. The latter stress circle represents the stresses in the sample at the end of the  
287 consolidation procedure (stress at steady state flow). It corresponds to the stress circle at the  
288 end of consolidation **in** the uniaxial compression test.

289 In addition to the above shear **testing, powder** aeration tests were performed, allowing  
290 consideration of the fluidisation capability of the studied powders. **The** aeration ratio **was**  
291 **found to range** from 32.4 for whey to 12.7 (demineralised whey) and 8.98 for **skimmed**  
292 **milk, whereas the** aerated **energy varied** from 4.8 mJ (whey) to 10.1 mJ (demineralised  
293 whey) and 14.4 mJ (**skimmed** milk). **The** aeration data **indicated** that **whey showed the**  
294 **lowest cohesion of all the samples tested, i.e.** highest aeration **ratio** in combination with the  
295 lowest aerated energy. All **the** tested powders **exhibited** complete fluidisation **at 4** mm/s air  
296 **velocity, with** basic flowability energy ranging from 127 mJ (**skimmed** milk and  
297 demineralised whey) to 157 mJ for whey.

298

## 299 **Conclusions**

300

301 **The results showed that the surface energy of the studied milk product powders was**  
302 **dominated by the dispersive component, indicating their low polarity character.** Surface  
303 energy profiles of **skimmed** milk and demineralised whey **showed a characteristic steep**  
304 exponential decrease of the surface energy from approximately 170 mJ/m<sup>2</sup> to 60 mJ/m<sup>2</sup>  
305 (demineralised whey) and of 140 mJ/m<sup>2</sup> to 45 mJ/m<sup>2</sup> (**skimmed milk**), **reflecting the**  
306 relatively **small** number of high energy sites located at the surface of the studied materials.  
307 **From 5% up to 20% surface coverage, the surface energy profiles reached a plateau** at 45  
308 mJ/m<sup>2</sup> for **skimmed** milk and 60 mJ/m<sup>2</sup> for demineralised **whey**. **Whey** powder surface  
309 energy coverage dependence exhibited stable non-exponential (linear) pattern with the  
310 magnitude of the observed surface energy approximately 45 mJ/m<sup>2</sup>, thus reflecting high  
311 homogeneity of acting energetic surface sites. For all three tested materials, **the polar**  
312 component of the surface energy was negligible in comparison to the dispersive component. It  
313 was **found that** the polar surface active sites **were** of relatively low energy in all **the** studied  
314 powders, **confirming** their low polarity character. **The observed** dispersive surface energy  
315 **showed characteristically broad** distributions for **skimmed** milk and demineralised whey  
316 ranging from 40 mJ/m<sup>2</sup> to **175** mJ/m<sup>2</sup> and **120** mJ/m<sup>2</sup>, **respectively**, thus reflecting **the large**  
317 number of structural elements responsible for this behaviour. **In contrast, the dispersive**  
318 surface energy distribution **of whey was very narrow, ranging from only** 42.8 mJ/m<sup>2</sup> to 45  
319 mJ/m<sup>2</sup>. **The macroscopic** powder flow behaviour of **the** studied materials **was analysed by**  
320 **examining the** yield locus and flow function dependencies at different stress levels. **The**  
321 **determined** yield locus and Mohr's circles **indicated** that demineralised whey exhibited free  
322 flowing powder characteristics (observed friction coefficient 11.7). However, **the friction**

323 coefficients of **the skimmed** milk and whey powders were in the **range 3.3** to 4.5, **which are**  
324 values characteristic for cohesive **powders**. All tested powders **allowed** complete fluidisation  
325 **at 4 mm/s** air **velocity**, **with** basic flowability **energies** ranging from 127 mJ (**skimmed** milk  
326 and demineralised whey) to 157 mJ for whey.

327

### 328 **Acknowledgements**

329 Financial support from the Operational Program Research and Development for Innovations –  
330 European Regional Development Fund (grants CZ.1.05/3.1.00/14.0302 and  
331 CZ.1.05/2.1.00/03.0058) and **the** Tomas Bata University in Zlin and Palacky University in  
332 Olomouc Internal Grant Agencies (projects IGA/FT/2014/001 and PrF\_2014\_032) is  
333 gratefully acknowledged. Special thanks to Mgr. K. Šafařová, Ph.D. for **performing the SEM**  
334 measurements.

335

### 336 **References**

- 337 Belgacem, M.N., Gandini, **A.**, & Pefferkorn, M.N. (1999). Interfacial phenomena in chro-  
338 matography. New York: Marcel Dekker.
- 339 Berlin, E., Howard, **N.M.**, & Pallansch, M.J. (1964). Specific surface area of milk powders  
340 produced by different drying methods. *Journal of Dairy Science*, **47**, **132–138**.
- 341 Bolenz, S., Romisch, **J.**, & Wenker, T. (2014). Impact of amorphous and crystalline lactose  
342 on milk chocolate properties. *International Journal of Food Science and Technology*, **49**,  
343 **1644–1653**.

344 Collins, M.N. (2014). Hyaluronic acid biomedical and pharmaceutical applications.  
345 Shawbury: Smithers Rapra.

346 Crowley, S.V., Gazi, I., Kelly, A.L., Huppertz, T., & O'Mahony, J.A. (2014). Influence of  
347 protein concentration on the physical characteristics and flow properties of milk protein  
348 concentrate powders. *Journal of Food Engineering*, **135**, 31–38.

349 Dorris, G.M., & Gray, D.G. (1980). Adsorption of normal-alkanes at zero surface coverage  
350 on cellulose paper and wood fibers. *Journal of Colloid and Interface Science*, **77**, 353–362.

351 Fox, P.F., & McSweeney, P.L.H. (1998). Dairy chemistry and biochemistry. New York:  
352 Kluwer Academic/Plenum Publishers.

353 Gajdošíková, R., Lapčíková, B., & Lapčík, L. (2011). Surface phenomena and wetting of  
354 porous solids. *Physical Chemistry: An Indian Journal*, **6**, 146–162.

355 Gamble, J.F., Leane, M., Olusanmi, D., Tobyn, M., Supuk, E., Khoo, J., & Naderi, M.  
356 (2012). Surface energy analysis as a tool to probe the surface energy characteristics of  
357 micronized materials – a comparison with inverse gas chromatography. *International Journal  
358 of Pharmaceutics*, **422**, 238–244.

359 Gauchon, F., Famelart, M.H., Mariette, F., Raulot, K., Michel, F., & LeGraet, Y. (1997).  
360 Combined effects of temperature and high-pressure treatments on physicochemical  
361 characteristics of skim milk. *Food Chemistry*, **59**, 439–447.

362 Helaine, B.J., Valdemiro, C.S., Dias, N.F.G.P., Borges, P., & Tanikawa, C. (2001). Impact of  
363 different dietary protein on rat growth, blood serum lipids and protein and liver cholesterol.  
364 *Nutrition Research*, **21**, 905–915.

365 Hoffman, **J.R.**, & Falvo, M.J. (2004). Protein – Which is best? *Journal of Sports Science and*  
366 *Medicine*, **3**, **118** **130**.

367 Jensen, R.G., Ferris, **A.M.**, & Lammi-Keefe, C.J. (1991). The composition of milk fat.  
368 *Journal of Dairy Science*, **74**, **3228** **3243**.

369 Lapčík, L., Lapčík, L., De Smedt, S., Demeester, **J.**, & Chabreček, P. (1998). Hyaluronan.  
370 preparation, structure, properties and applications. *Chemical Reviews*, **98**, **2663** **2684**.

371 Lapčík, L., Lapčík, L., Kubiček, P., Lapčíková, B., Zbořil, **R.**, & Nevěčná, T. (2014) Study  
372 of penetration kinetics of sodium hydroxide aqueous solution into wood samples.  
373 *BioResources*, **9**, **881** **893**.

374 Lapčík, L., Lapčíková, B., Krásný, I., Kupská, I., Greenwood, **R.W.**, & Waters, K.E. (2012).  
375 Effect of low temperature air plasma treatment on **wetting** and flow properties of kaolinite  
376 powders. *Plasma Chemistry and Plasma Processing*, **32**, **845** **858**.

377 Lapčík, L., Otyepková, E., Lapčíková, **B.**, & Otyepka, M. (2013). Surface energy analysis  
378 (SEA) study of hyaluronan powders. *Colloids and Surfaces A: Physicochemical and*  
379 *Engineering Aspects*, **436**, **1170** **1174**.

380 Lazar, P., Otyepková, E., Banaš, P., Fargašová, A., Šafářová, K., Lapčík, L., Pechoušek,  
381 Zbořil, **R.**, & Otyepka, M. (2014). The nature of high surface energy sites in graphene and  
382 graphite. *Carbon*, **73**, **448** **453**.

383 Manso, **M.A.**, & Lopez-Fadino, R. (2004). j-Casein macropeptides from cheese whey:  
384 Physicochemical, biological, nutritional, and technological features for possible uses. *Food*  
385 *Reviews International*, **20**, **329** **355**.



386 Martinez-Padilla, L.P., Garcia-Mena, V., Casas-Alencaster, **N.B.**, & Sosa-Herrera, M.G.  
387 (2014). Foaming properties of skim milk powder fortified with milk proteins. *International*  
388 *Dairy Journal*, **36**, **21** **28**.

389 Mocanu, A.M., Moldoveanu, C., Odochian, L., Paius, C.M., Apostolescu, **N.**, & Neculau, R.  
390 (2012). Study on the thermal behaviour of casein under nitrogen and air atmosphere by means  
391 of the TG-FTIR technique. *Thermochimica Acta*, **546**, **120** **126**.

392 Mohammadi-Jam, **S.**, & Waters, K.E. (2014). Inverse chromatography applications: A  
393 review. *Advances in Colloid and Interface Science*,  
394 <http://dx.doi.org/10.1016/j.cis.2014.07.002>.

395 Nilufer-Erdil, D., Serventi, L., Boyacioglu, **D.**, & Vodovotz, Y. (2012). Effect of soy milk  
396 powder addition on staling of soy bread. *Food Chemistry*, **131**, **1132** **1139**.

397 Osorio, J., Monjes, J., Pinto, M., Ramirez, **C.**, **Simpson, R.**, & Vega, O. (2014). Effects of  
398 spray drying conditions and the addition of surfactants on the foaming properties of a whey  
399 protein concentrate. *LWT-Food Science and Technology*, **58**, **109** **115**.

400 Raemy, A., Hurrell, **R.F.**, & Löliger, J. (1983). Thermal behavior of milk powders studied by  
401 differential thermal analysis and heat flow calorimetry. *Thermochimica Acta*, **65**, **81** **92**.

402 Rahman M.S., Al-Hakmani, H., Al-Alawi, **A.**, & Al-Marhubi, I. (2012). *Thermochimica Acta*,  
403 **549**, **116** **123**.

404 Ranken, M.D., Kill, **K.C.**, & Baker, C. (1997). **Food industrial manual**. London: Blackie  
405 Academic & Professional.

406 Romeih, E.A., Abdel-Hamid, **M.**, & Awad, A.A. (2014). The addition of buttermilk powder  
407 and transglutaminase improves textural and organoleptic properties of fat-free buffalo yogurt.  
408 *Dairy Science & Technology*, **94**, 297 309.

409 Saffari, **M.**, & Langrish, T. (2014). Effect of lactic acid in-process crystallization of  
410 lactose/protein powders during spray drying. *Journal of Food Engineering*, **137**, 88 94.

411 Schultz, L., Lavielle, **C.**, & Martin, J. (1987). The role of **the** interface in carbon fibre-epoxy  
412 composites. *Journal of Adhesion*, **23**, 45 60.

413 Tamime, A.Y., Robinson, **R.K.**, & Michel, M. (2007). Microstructure of concentrated and  
414 dried milk products. In A.Y. Tamime (Ed.), *Structure of dairy products* (pp. 104 133).  
415 Oxford: Blackwell Publishing Ltd.

416 Vuataz, G., Meunier, **V.**, & Andrieux, J.C. (2010). Tg-DTA approach for designing reference  
417 methods for moisture content determined in food powders. *Food Chemistry*, **122**, 436 442.

418 Zhou, P., Liu, D.S., Chen, X.X., Chen, **Y.J.**, & Labuza, T.P. (2014). Stability of whey protein  
419 hydrolysate powders: Effects of relative humidity and temperature. *Food Chemistry*, **150**,  
420 457 462.

421

422 **Figures captions**

423

424 Figure 1. SEM images of studied powders: A) skimmed milk, B) **whey**, and C) demineralised  
425 whey.

426 Figure 2. Thermogravimetric **analysis of** studied powder milk products: full line – **powdered**  
427 skimmed milk, **dotted** line **powdered** whey, short dashed line – demineralised **powdered**  
428 whey.

429 Figure 3. DSC pattern of studied powder milk products: full line – **powdered** skimmed milk,  
430 dot line – **powdered** whey, short dashed line – demineralised **powdered** whey.

431 Figure 4. Surface energy and its **component** profiles **of powdered** milk products: circle –  
432 **powdered** whey, **triangle** – demineralised **powdered** whey, diamond – **powdered skimmed**  
433 **milk**, **black**– dispersive component of the surface energy (SFE), **red** polar component of  
434 **SFE**, **green** colour – total SFE.

435 Figure 5. Dispersive surface energy distribution **of** demineralised **powdered** whey (circle),  
436 **powdered skimmed** milk (triangle down) and **powdered** whey (triangle up). **Inset:**  
437 **expanded** dispersive surface energy distribution **of** whey sample.

438 Figure 6. Yield locus and Mohr's circles of studied **powdered** milk products: full square –  
439 **skimmed** milk, full triangle up whey, empty circle demineralised whey (measured at 24  
440 °C).

441

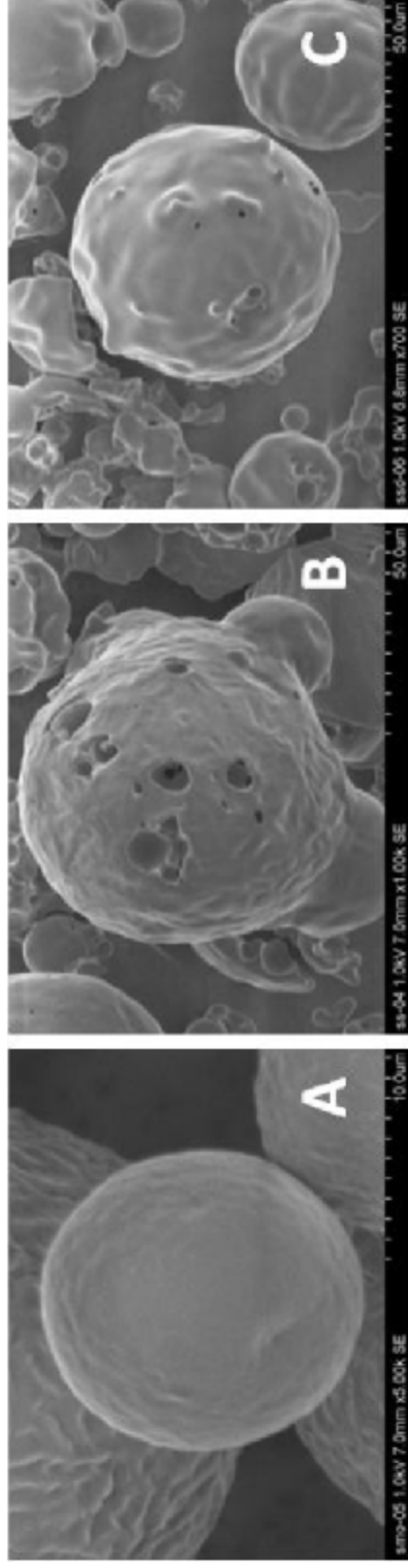


Figure 1. SEM images of studied powders: A) skimmed milk, B) whey, and C) demineralised whey.

Figure(s)

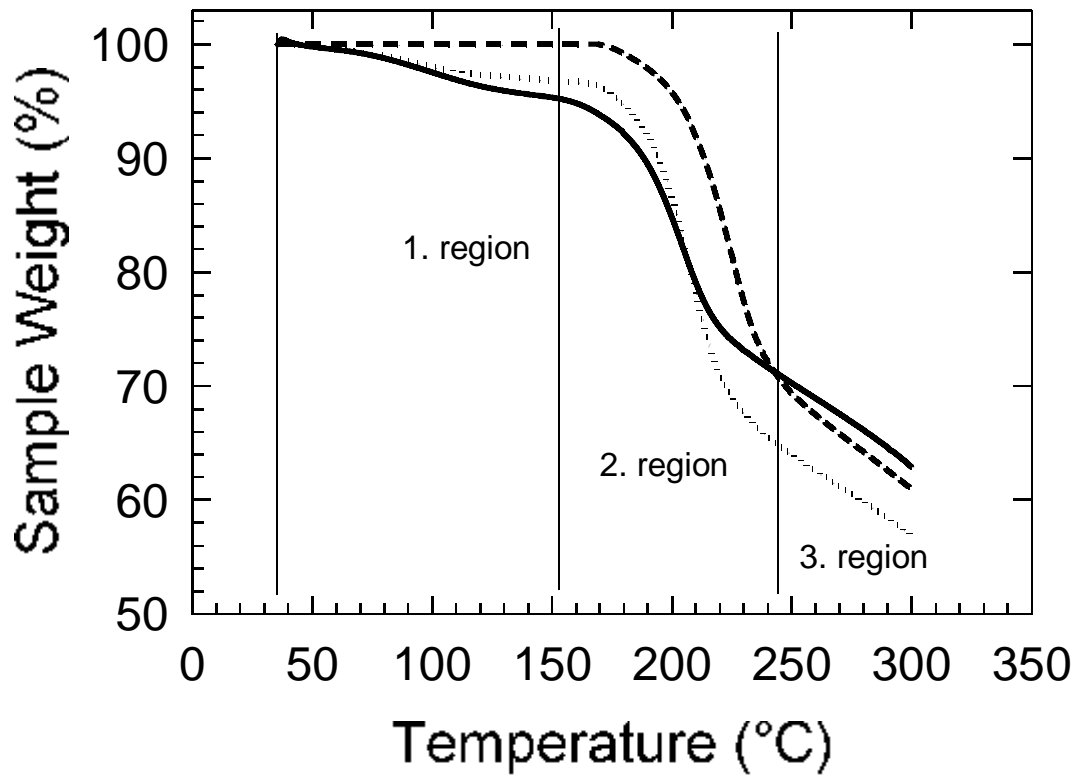


Figure 2. Thermogravimetric analysis of studied powder milk products: full line – powdered skimmed milk, dotted line powdered whey, short dashed line – demineralised powdered whey.

Figure(s)

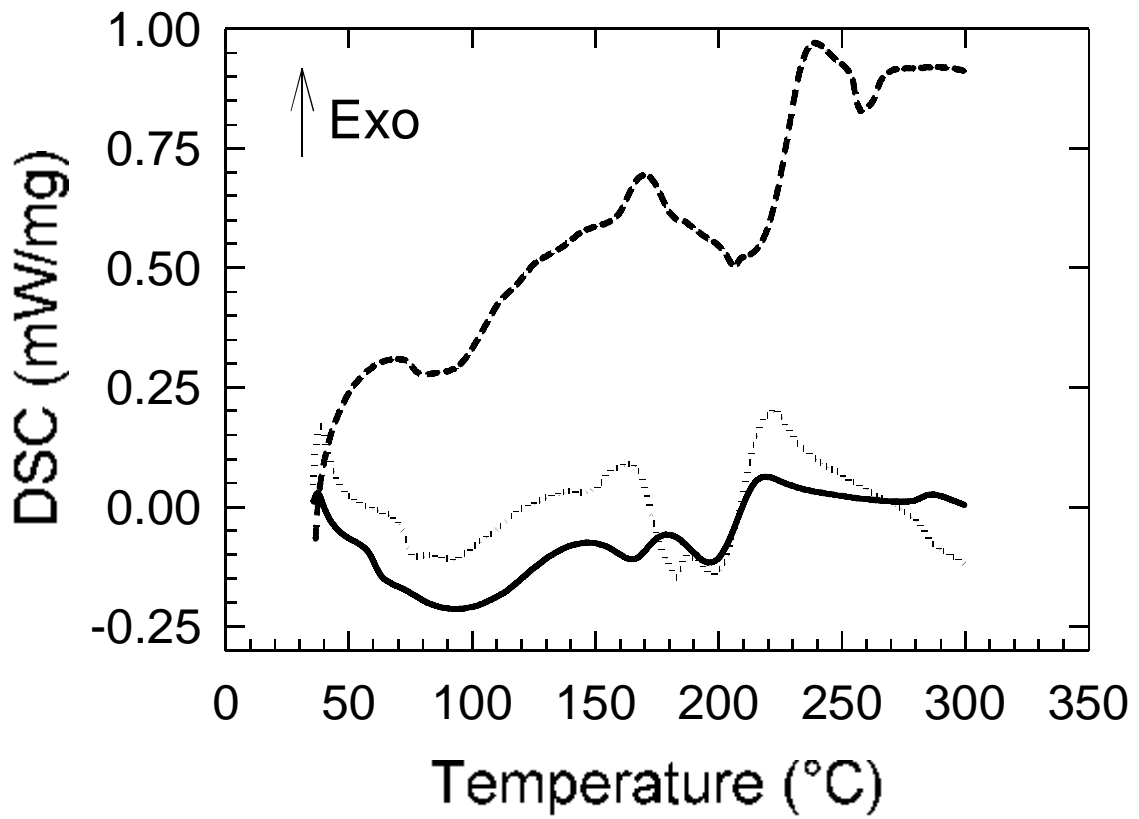


Figure 3. DSC pattern of studied powder milk products: full line – **powdered** skimmed milk, dot line – **powdered** whey, short dashed line – demineralised **powdered** whey.

Figure(s)

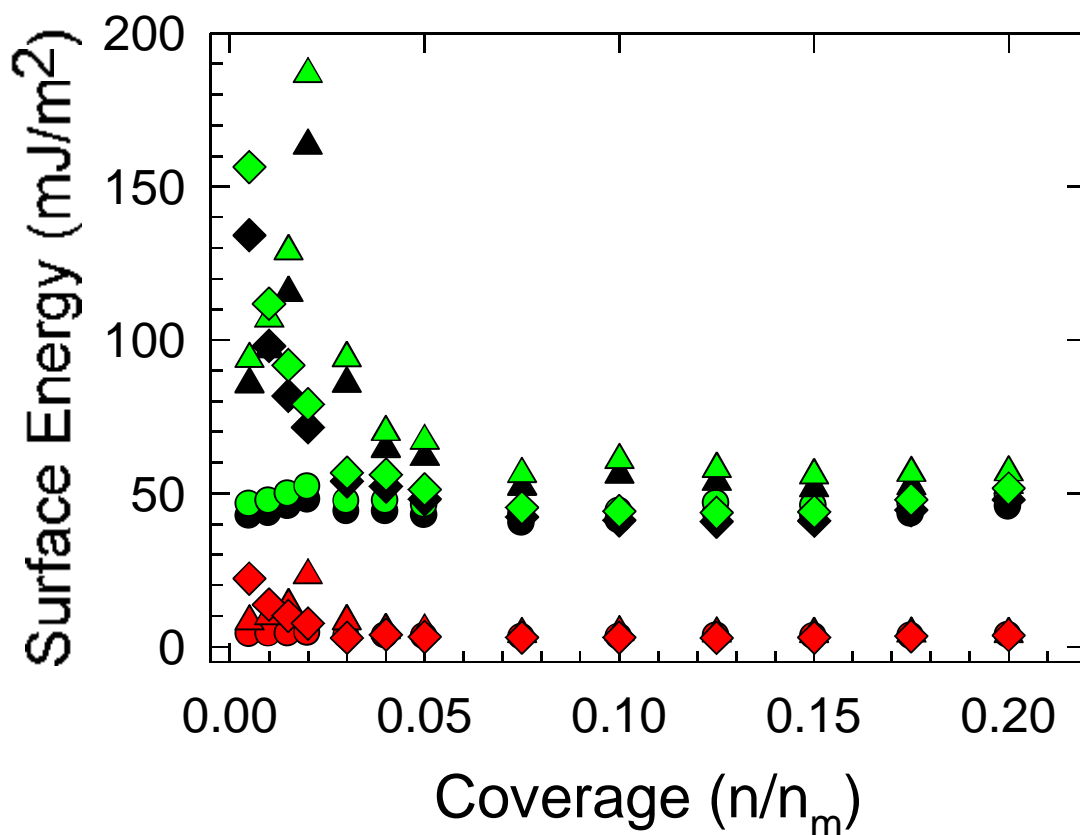


Figure 4. Surface energy and its **component** profiles of **powdered** milk products: circle – **powdered** whey, **triangle** – demineralised **powdered** whey, diamond – **powdered** skimmed **milk**, **black**– dispersive component of the surface energy (SFE), **red** polar component of SFE, **green** colour – total SFE.

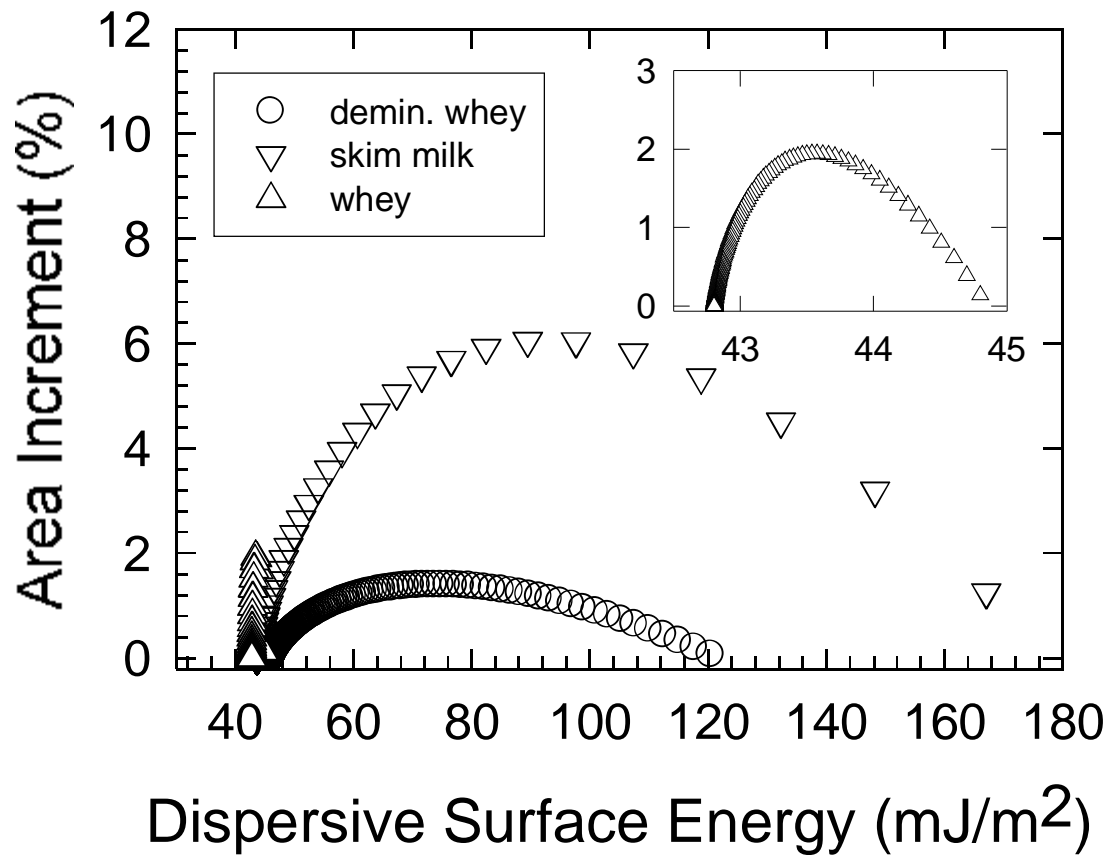


Figure 5. Dispersive surface energy distribution of demineralised powdered whey (circle), powdered skimmed milk (triangle down) and powdered whey (triangle up). **Inset:** expanded dispersive surface energy distribution of whey sample.



Figure(s)

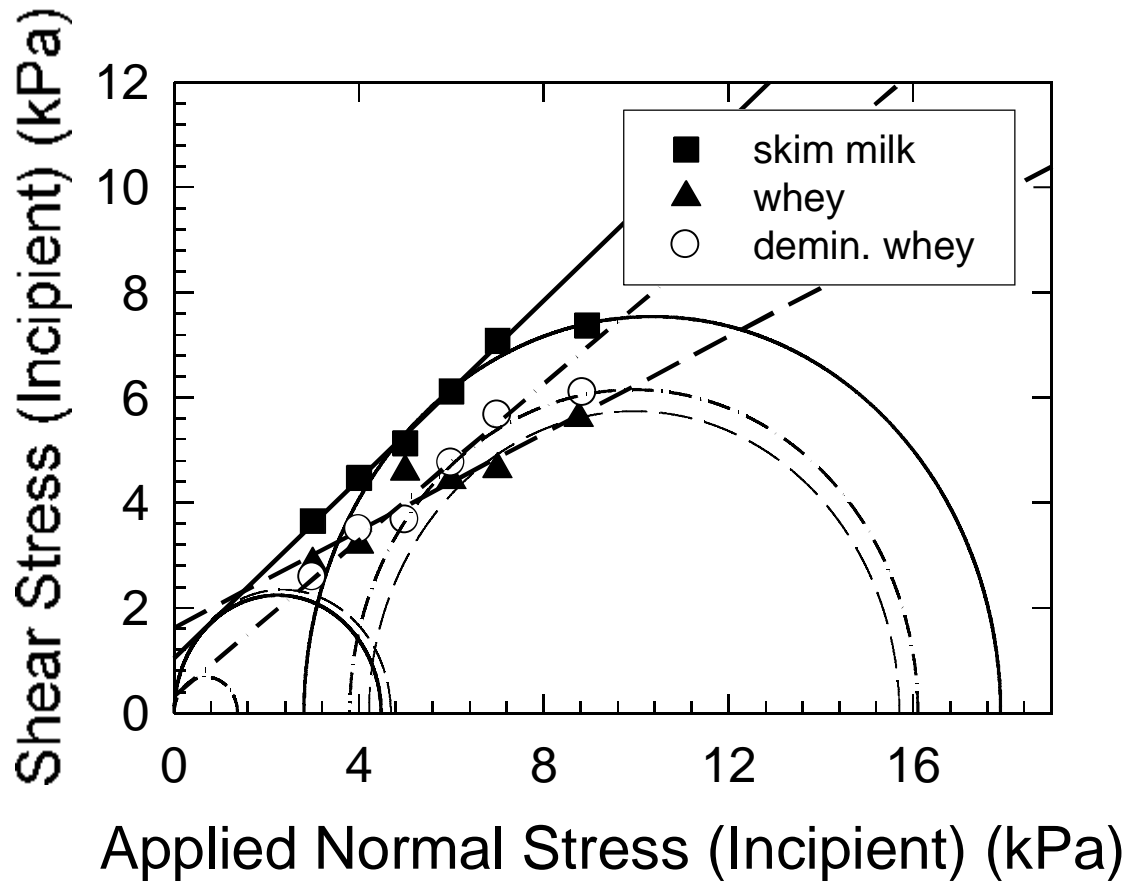


Figure 6. Yield locus and Mohr's circles of studied **powdered** milk products: full square **skimmed** milk, full triangle up – whey, empty circle – demineralised whey (measured at 24 °C).